Kidney International, Vol. 68 (2005), pp. 2726–2734

Constriction velocities of renal afferent and efferent arterioles of mice are not related to SMB expression

Andreas Patzak, Daria Petzhold, Thomas Wronski, Peter Martinka, Gopal J. Babu, Muthu Periasamy, Hannelore Haase, and Ingo Morano

University Medicine Charité, Johannes-Müller-Institute for Physiology, Berlin, Germany; Max Delbrück Centrum for Molecular Medicine, Molecular Muscle Physiology, Berlin, Germany; and Department of Physiology and Cell Biology, College of Medicine and Public Health, The Ohio State University, Columbus, Ohio

Constriction velocities of renal afferent and efferent arterioles of mice are not related to SMB expression.

Background. Constriction of renal arterioles contributes significantly to the control of perfusion and glomerular filtration. Afferent but not efferent arterioles express smooth muscle myosin heavy chain B (SMB) (with a 5′-insert of seven amino acids). The aim of the present study was to investigate (*1*) the constriction characteristics of afferent and efferent arterioles under physiologic load and (*2*) whether expression of SMB may causally contribute to these constriction characteristics.

Methods. We compared constriction parameters [constriction amplitude, maximal rate of constriction velocity ("dc/dt_{max}"), and time to half-maximal constriction ($t_{1/2}$) of in vitro perfused renal afferent and efferent arterioles of wild-type (smb(+/+)] and homozygous SMB knockout [smb(−/−)] mice upon stimulation with angiotensin II (Ang II) (10^{-8} mol/L) and potassium chloride (KCl) (100 mmol/L). SMB expression was investigated by double-labeling immunofluorescence.

Results. Contraction amplitude and dc/dt_{max} of mouse afferent arterioles upon Ang II stimulation were significantly greater compared to efferent arterioles. However, constriction amplitudes, dc/dt_{max}, and $t_{1/2}$ of afferent as well as efferent arterioles upon Ang II stimulation were similar in smb(+/+) and smb(−/−) mice. Constriction amplitudes upon KCl stimulation of afferent arterioles were similar in both smb(+/+) and smb(−/−) mice. Furthermore, KCl-induced dc/dt_{max} and $t_{1/2}$ of afferent arterioles were similar in both smb(+/+) and smb(−/−) mice. SMB expression could be detected in afferent but not efferent arterioles in smb(+/+) mice. No SMB expression in either arteriole could be observed in smb(−/−) mice.

Conclusion. Our results suggest that the presence of different alternatively 5′-spliced smooth muscle-myosin heavy chain (SM-MHC) isoforms does not dominate the different contractile features of physiologically loaded renal afferent or efferent arterioles.

Key words: afferent arteriole, efferent arteriole, smooth muscle, myosin heavy chains, juxtaglomerular apparatus.

Received for publication March 1, 2005
and in revised form May 9, 2005
Accepted for publication July 7, 2005

Type II myosin is the molecular motor which causes smooth muscle cell (SMC) contraction by cyclic interaction with actin and hydrolysis of adenosine triphosphate (ATP). The native myosin II consists of two heavy chains (myosin heavy chain, MHC) with around 200 kD each, which revealed a 140 nm alpha-helical "rod" domain and a pear-shaped N-terminal "head" domain with around 20 nm length. Two pairs light chains (myosin light chain, MLC) with 17 kD (essential MLC) and 20 kD (regulatory MLC) are noncovalently associated with each MHC close to the head domain [1, 2].

Three different MHC genes are expressed in SMCs, namely, SM-MHC as well as MHC which are also expressed in nonmuscle (NM) cells (NM-MHCA and NM-MHCB [3–5]). SM-MHC is exclusively expressed in SMCs and located on the human chromosome 16p13.13 [6]. Various MHC isoenzymes have distinct functions in SMCs. They form different contractile systems which are recruited during phasic contraction (the SM-MHC) or during tonic contraction upon sustained activation (the NM-MHC isoenzymes) [7, 8].

The SM-MHC gene transcript is alternatively spliced at both the 3′-(carboxy-terminal myosin tail) and at the 5′-end (amino-terminal head domain). Inclusion of a 39 nucleotide exon which encodes nine amino acids at the most 3′-terminus generates the translation of a SM-MHC isoenzyme with 1443 amino acids and around 200 kD (SM2) with a shortened tail region. Exclusion of this exon causes the translation of an elongated tail with 1477 amino acids and around 204 kD (SM1), containing a nonhelical tailpiece domain with a phosphorylatable serine residue [9–11].

5′-splicing of SM-MHC is accomplished by excision of a highly conserved exon with 21 nucleotide (seven amino acids) causing a shortened flexible surface loop (loop 1) close to the ATP-binding 25K/50K junction [12–14]. SM-MHC without the 5′-insert were designated as "SMA" isoforms (SM1A and SM2A), those with 5′-insert as "SMB" forms (SM1B and SM2B).

Alternative 3′-splicing in the carboxy terminus of SM-MHC isoforms seems not to be associated with motor properties of myosin [15] or shortening velocity of smooth muscle preparations [16]. However, alternatively 5′-spliced myosin isoenzymes revealed different kinetic and conferred distinct contractile features to muscle preparations. Due to the proximity to the ATP binding pocket, the length of loop 1 may regulate the rate of adenosine diphosphate (ADP) release from the catalytic domain and, therefore cross-bridge detachment [17], thus determining V_{max} [18] and the duration of the duty cycle [19]. In fact, SMB (with 5′-insertion and elongated loop 1) revealed a reduced duration of the duty cycle, increased shortening velocity as well as increased actin-activated ATPase activity and velocity of actin filament sliding in the in vitro motility assay [13, 20, 21]. In a recently generated knockout mouse model with targeted ablation of exon 5b [22], the SMA isoenzymes were the sole expressed SM-MHC isoenzymes which conferred decreased contraction kinetics to smooth muscle preparations. In the same animal model, addition of magnesium ADP (MgADP) revealed a stronger effect on the force-generating states of SMA [15], supporting the hypothesis that a shorter loop 1 releases ADP slower and increases the duration of the duty cycle. Please note, however, that results of these studies reflect the kinetic features of myosin in vitro or under unloaded rather than under physiologically loaded conditions.

Renal afferent and efferent arterioles express different alternatively 5′- and 3′-spliced MHC isoforms. Afferent arterioles expressed SM1, SM2, SMA, and SMB, while efferent arterioles expressed mainly SM1 and SMA [23, 24]. In a recent study [24], SMB expression in afferent arterioles was associated with enhanced constriction velocity of afferent arterioles upon angiotensin II (Ang II) or norepinephrine stimulation. However, it is not clear, whether the presence of SMB or the different microstructures and responsiveness to Ang II and norepinephrine [25, 26] of renal afferent and efferent arterioles are mainly responsible for the different constriction velocities. To answer this question, we examined Ang II responsiveness of efferent arterioles and the Ang II and KCl responsiveness of afferent arterioles of wild-type [smb(+/+)] and homozygous SMB knockout [smb(−/−)] mice. While there was a significant difference of Ang II–induced constriction amplitude and velocity between renal afferent and efferent arterioles, we did not observe any significant difference of constriction parameters of afferent and efferent arterioles between smb(+/+) and smb(−/−) mice.

METHODS

Animal model

We used a homozygous SMB knockout mouse model (smb−/−) which has been recently introduced [22]. The homozygous SMB knockout and the corresponding wild-type mice (smb+/+) were generated by breeding heterozygous SMB knockout mice. Animals were fed with standard mouse chow and allowed free access to tap water. All animal procedures adhered to the guidelines for care and handling of animals established by the United States Department of Health and Public Services and published by the National Institutes of Health.

Constriction studies of renal afferent and efferent arterioles

Physiologic salt solution (PSS) was used with the following composition: NaCl 115, $NaHCO_3$ 25, K_2HPO_4 2.5, $CaCl_2$ 1.3, $MgSO_4$ 1.2, and glucose 5.5 (mmol/L). The KCl solution consisted of 100 mmol/L KCl, whereby 95 mmol/L NaCl were substituted by KCl. Dulbecco's modified Eagle's medium (DMEM) (1000 mL) was supplied with 100 mg streptomycin, and 100000 U penicillin. The bicarbonate buffered solution was equilibrated with 5% CO_2 and 95% O_2. The pH was adjusted to 7.4 after addition of bovine serum albumin (BSA). The oxygen partial pressure was below 200 mm Hg in the perfusion and bath solution during the experiment. The pH was stable. The concentration of BSA in DMEM, which was used for dissection, and in PSS (bath solution) was 0.1%. The perfusate of the arterioles consisted of PSS with a BSA concentration of 1%. BSA was obtained from SERVA Electrophoresis (Heidelberg Germany). Ang II, DMEM, streptomycin, and penicillin were from Sigma-Aldrich (München, Germany).

Male mice (body mass was 21 to 33 g and age was between 12 and 15 weeks) were used in this study. After killing the animal, the kidneys were immediately removed and sliced along the corticomedullary axis. The arterioles were prepared at 4°C in DMEM, which was enriched with 0.1% albumin. The dissection procedure of the afferent and efferent arterioles was the same as described before [27]. The macula densa, the adjacent parts of the tubule, and the glomerulus were preserved. In case of the dissection of an afferent arteriole the efferent arteriole was removed by cutting close to the glomerulus. The same was done with the afferent arteriole when using the efferent arteriole for the experiment. This assured standard conditions in regard to the total vascular resistance of preparation, and consequently the flow. The preparation was transferred into a thermoregulated chamber (volume 1.5 mL) (VETEC, Rostock, Germany) on a stage of an inverted microscope (Axiovert 100) (Carl Zeiss, Oberkochen, Germany). The perfusion system allowed movement and adjustment of concentric, holding and perfusion pipettes (Luigs & Neumann, Ratingen, Germany). The pipettes were made by customizing glass tubes (Drummond Scientific Company, Broomall, PA, USA). The holding pipette into which the free end of the arteriole was aspirated had an aperture of roughly 26 μm at the tip and a constriction of about 20 μm. The inner

perfusion pipette with an aperture of 5 μm was advanced into the lumen of the arteriole. The perfusion pipette was connected to a reservoir containing the perfusion solution and to a manometer. Afferent arterioles were perfused from the free end with a pressure of 80 mm Hg in the pressure head. Efferent arterioles were perfused retrograde from the free, cut end with a pressure of 60 mm Hg. To test the autoregulatory behavior of the afferent arterioles we measured the response of afferent arterioles diameter to stepwise increased pressure. The diameter of afferent arterioles increased nonlinearly with increasing pressure. The pressure-diameter curve showed a flat course for most of the investigated afferent arterioles for pressures higher than 80 mm Hg in the pressure head. We conclude from this course that we are at the lower end of the physiologic pressure range when using a pressure of 80 mm Hg in this perfusion setup. The value of the pressure depends on the size and length of the tubes and the perfusion pipette located between the pressure head and the arterioles. Therefore, pressure-diameter curves are determined for each experimental setup. If perfusion was not achieved within 90 minutes after the mouse was killed, the experiment was terminated. Twenty minutes were allowed for adaptation after starting perfusion and gradual heating. Only arterioles with a remaining basal tone were used. Hypoxic or otherwise injured vessels were readily identified by pronounced vasodilatation. The viability of the afferent arterioles was tested by applying 100 mmol/L KCl at the beginning of the experiment, which induced strong constrictions of afferent but not of efferent arterioles [cf., 28, 29]. Ten minutes after the viability test, the luminal diameters were recorded and the constriction experiments started. First, KCl, then Ang II–induced constrictions were investigated in each afferent arteriole. Only one arteriole was used from each animal.

Experimental protocols

The constriction of afferent arterioles was induced by depolarization of the preparations with a 100 mmol/L KCl solution applied from the bath side. Further, the constriction response to a bolus application of Ang II of afferent and efferent arterioles was determined by applying Ang II in a concentration of 10^{-8} mol/L from the bath side. Since KCl and Ang II induce constriction via different pathways, the comparison of the contractile responses between the two stimuli gives an idea about their influence on the observed contractile properties. KCl and Ang II were always given in the same order, first, KCl, then Ang II in afferent arterioles. Pilot experiments did not show any effect of the KCl constriction on Ang II effects or vice versa. There were only one KCl and one Ang II application in each arteriole.

Signals were recorded on SVHS video tapes (video recorder AG-MD 830) (Panasonic, Kadoma City, Japan). The magnification results from an objective (×40) (Carl Zeiss) and projection (×1) on a 0.3 inch chip digital camera (CB-3803S) (GKB, Tai Chung, Taiwan). Video sequences were digitized using a frame grabber card (UDT 55-LC-EZ-50) (Data Translation, Marlboro, MA, USA). Pictures were taken every 300 mseconds and the vessel diameters were determined using a customized software (Dr. H. Siegmund, Johannes-Müller-Institute of Physiology, Humboldt-University of Berlin, Germany). The equipment allowed a resolution of 0.2 μm of the vessel structures. The luminal diameter of the arterioles was determined for each picture. These data served for analysis of the course of the constriction after KCl and Ang II application, including the time to half-maximal constriction ($t_{1/2}$). Further, the maximum of the constriction velocity was assessed using a customized software (Dr. T. Wronski, Johannes-Müller-Institute of Physiology, Humboldt-University of Berlin, Germany). The time series were smoothed by applying a moving average (three-point window). Then, the first deviation of the averaged curve was calculated, which served for the assessment of the maximum constriction velocity (dc/dt_{max}).

Immunfluorescence analysis of SM-MHC isoforms

Cryostat sections 5 μm thick were prepared with a Jung CM 2200 cryostat (Leica, Wetzlar, Germany). Sections were fixed in 4% formaldehyde in 0.1 mol/L phosphate buffer, pH 7.4, for 15 minutes at room temperature. To suppress unspecific labeling, cryosections were preincubated in 20 mmol/L Tris-HCl, pH 8.4, 130 mmol/L NaCl, 0.05% Tween-20, 0.02% NaN_3, and 1% BSA for 20 minutes at room temperature. Immunolabeling was performed for 2 hours at 37°C with a rabbit anti-SMB antibody raised against the seven amino acid insert (QGPSFAY) (rat and mouse sequence) located at the 25K/50K junction of SM-MHC (aSMB) (0.05 to 7.5 μg/mL), with previously shown specificity [30], and antismooth muscle actin antibody (clone asm-1) (Boehringer, Mannheim, Germany) (0.5μg/mL). For immunodetection, primary antibodies were visualized by staining with Alexa-conjugated species-specific secondary antibodies (Alexa488 and Alexa594) (Molecular Probes, Leiden, The Netherlands) (diluted 1:1000) for 1 hour at 37°C. Primary and secondary antibodies were diluted in 20 mmol/L Tris-HCl, pH 8.4, 130 mmol/L NaCl, 0.05% Tween-20, 0.02% NaN_3, and 1% BSA. Immunolabeling was evaluated with an Axioplan fluorescence microscope (Carl Zeiss) using appropriate filter systems and a fluorescence imaging system (ColourView 12).

Immunofluorescence analysis of renin expression

Immunofluorescent staining for renin was performed on 10 μm thin cryosections of mouse kidneys, which were

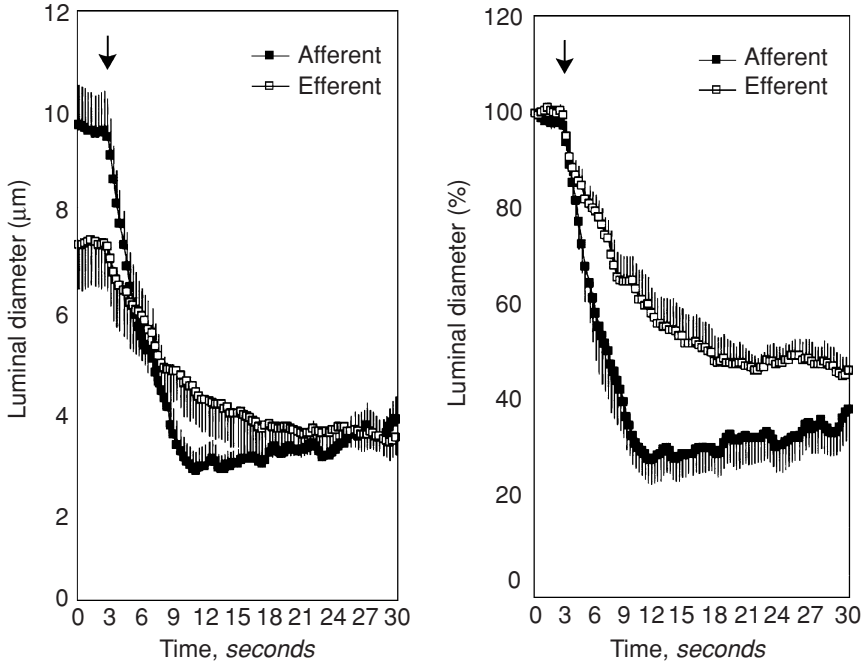

Fig. 1. Comparison of the time courses of the angiotensin II (Ang II)–induced (10^{-8} mol/L) constriction of afferent ($N = 9$) and efferent ($N = 6$) arterioles in smb(+/+) mice. Absolute luminal diameters (left) differed significantly ($P < 0.05$) between both groups. Constriction amplitude of afferent arteriole (relative luminal diameter right) was significantly higher ($P < 0.05$). The arrows indicate the start of the constriction. Data are presented as mean ± SEM.

produced by slicing along the corticomedullary axis. Sections were fixed with 4% paraformaldehyde/phosphate-buffered saline (PBS) for 10 minutes and washed in PBS for 10 minutes. Unspecific binding of the antibodies was prevented by incubation of sections with blocking solution containing 3% BSA and 0.1% Triton-X100. Primary rabbit antirenin antibody was a generous gift of Professor Tadashi Inagami (Vanderbilt University, Nashville, TN, USA) and was used in the 1:300 dilution at 4°C overnight. After three consecutive 10-minute washing periods, the secondary fluorescein isothiocyanate (FITC)-labeled antirabbit antibody (Merck Biosciences, Darmstadt, Germany) was used in 1:500 dilution for 2 hours at room temperature. Slides were mounted with Vectashield-4′,6-diamino-2-phenylindole (DAPI) (Vector Laboratories, Burlingame, CA, USA) and visualized using inverted fluorescence microscope (Axiovert A 100) (Carl Zeiss) and a fluorescence imaging system (MetaMorph(tm)) (Universal Imaging Corporation, Downingtown, PA, USA). The total magnification of the optical and imaging system (objective 4×, high-sensitivity digital camera, model 2.3.2) (Diagnostic Instruments, Sterling Heights, MI, USA) allowed the visualization of about one third of the total area of the renal cortex. The resolution of the grabbed pictures was 7.2 pixel/µm. Black and white pictures (eight-bit) were analyzed using the software ImageJ (National Institutes of Health, Bethesda, MD, USA). Fluorescent areas were detected by applying a binary threshold. The analysis included the calculation of the total fluorescent area, the average size of fluorescent dots, and the area fraction (percentage of the total fluorescent area in relation to the total area of the field). Three slides, which were cut with a distance of 100 µm, were analyzed in each animal. The median of the three values of the parameters was used for further statistical analysis.

Statistics

The Brunner test for nonparametric analysis of longitudinal data was used to test for time-dependent changes in the arteriolar diameter [one-way analysis of variance (ANOVA)], to test for differences in the luminal diameters between the groups, and to check for differences in the time-dependent changes in diameter between the groups (two-way ANOVA). The Wilcoxon test for nonpaired data was applied for the comparison of independent measurements of the dc/dt_{max}, $t_{1/2}$, and parameters of the immunofluorescence analysis of renin expression. The same test was used for comparison of diameters of the different groups in the steady state during the control situation. Data are presented as mean ± SEM.

RESULTS

Different constriction kinetics of afferent and efferent arterioles of mouse kidney

The luminal diameters of efferent arterioles were smaller compared to afferent arterioles at the start of the experiment of wild-type animals [smb(+/+)] ($P < 0.05$) (Fig. 1). We observed statistically significant ($P < 0.05$) differences of the constriction features of efferent arterioles compared to afferent arterioles of smb(+/+). The time course of the constriction was flat in efferent arterioles in comparison with afferent arterioles (Fig. 1).

Table 1. Maximal rates of constriction velocities (dc/dt_{max}) and time to half-maximal constriction ($t_{1/2}$) of afferent and efferent arterioles of normal mice [smb(+/+)] and homozygous SMB knockout mice [smb(−/−)] upon angiotensin II (Ang II) and KCl stimulation.

	Ang II (10^{-8} mol/L)		KCl (100 mmol/L)
dc/dt_{max}	Afferent arteriole *μm/sec*	Efferent arteriole *μm/sec*	Afferent arteriole *μm/sec*
smb(+/+)	−3.0 ± 0.3 (9)[a]	−1.4 ± 0.2 (6)	−3.4 ± 0.4 (9)
smb(−/−)	−2.7 ± 0.4 (10)[a]	−1.3 ± 0.2 (8)	−3.7 ± 0.4 (11)
$t_{1/2}$	Afferent arteriole *seconds*	Efferent arteriole *seconds*	Afferent arteriole *seconds*
smb(+/+)	2.6 ± 0.5 (9)[a]	5.6 ± 1.4 (6)	3.5 ± 0.6 (9)
smb(−/−)	2.7 ± 0.4 (10)[a]	6.0 ± 0.8 (8)	3.6 ± 0.6 (11)

Values are mean ± SEM with the number of arterioles measured in parentheses.
[a] $P < 0.05$ comparing afferent versus efferent arterioles.

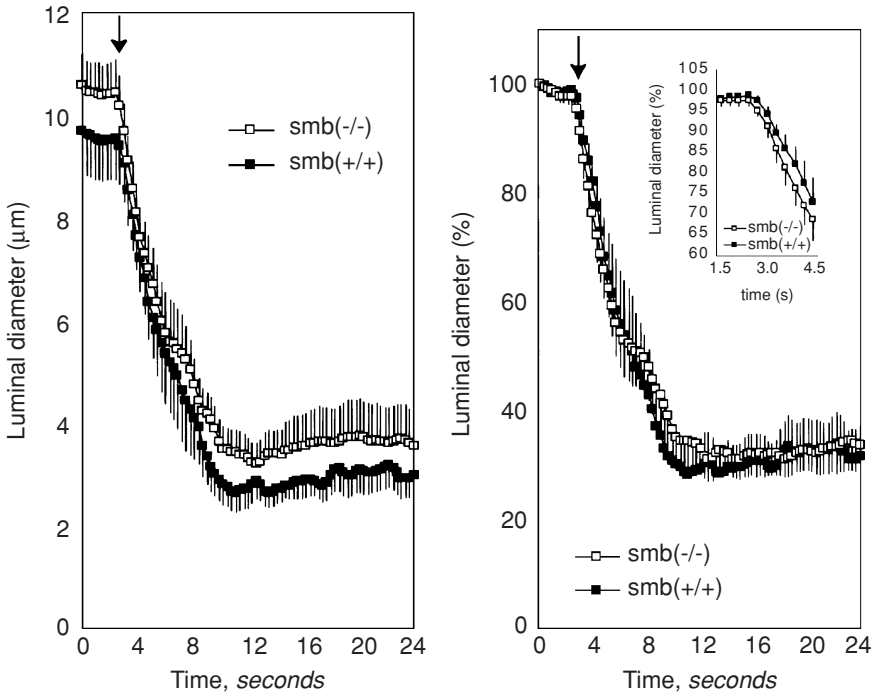

Fig. 2. Time courses of angiotensin II (Ang II) (10^{-8} mol/L)–induced constriction in isolated, perfused afferent arterioles in smb(−/−) ($N = 10$) and smb(+/+) mice ($N = 9$). Absolute diameters (μm, left panel) did not differ significantly between both groups. There were no differences in the Ang II response (see relative changes of luminal diameters, right panel). The arrows indicate the start of the constriction. The inserted graph on the right panel demonstrates the courses for the beginning of the constriction in higher time and amplitude resolution. Data are presented as mean ± SEM.

The maximum constriction velocity dc/dt_{max} of efferent arterioles was significantly ($P < 0.05$) smaller compared to afferent arterioles upon Ang II stimulation (Table 1). In addition, time to half-maximal constriction ($t_{1/2}$) of afferent arterioles was significantly ($P < 0.05$) smaller than $t_{1/2}$ of efferent arterioles upon Ang II stimulation (Table 1).

Loss of SMB did not alter the contractile features of afferent and efferent arterioles of mouse kidney

The complete ablation of the SMB isoform in smb(−/−) mice provided the opportunity to selectively investigate the physiologic role of 5′-spliced MHC isoenzymes by comparison of the constriction mechanics of renal arterioles of smb(−/−) with smb(+/+) mice. Control values of the luminal diameter of afferent and efferent arterioles were similar before the start of the constriction experiments in smb(−/−) and smb(+/+) mice (Figs. 2 to 4).

We compared the constriction amplitude, dc/dt_{max} as well as the $t_{1/2}$ of afferent arterioles of smb(+/+) and smb(−/−) mice to Ang II stimulation. Ang II (10^{-8} mol/L) applied from the bath side reduced the luminal diameter of afferent arterioles of smb(−/−) to a similar extent observed in smb(+/+) (Fig. 2). Furthermore, dc/dt_{max} and $t_{1/2}$ of afferent arterioles upon Ang II stimulation were similar in both groups (Table 1).

The same observation [i.e., no different contractile features between smb(+/+) and smb(−/−)] could be made with efferent arterioles. Luminal diameters prior the start of the experiment and constriction amplitudes (Fig. 3), dc/dt_{max} as well as $t_{1/2}$ upon Ang II stimulation were comparable in both mice groups (Table 1).

Furthermore, we determined the vasoconstriction responses of afferent arterioles to KCl depolarization. KCl elicited an almost complete constriction response (Fig. 4). This observation was similar in both smb(+/+) and smb(−/−). Please note that there were no differences of dc/dt_{max} and $t_{1/2}$ of afferent arterioles between

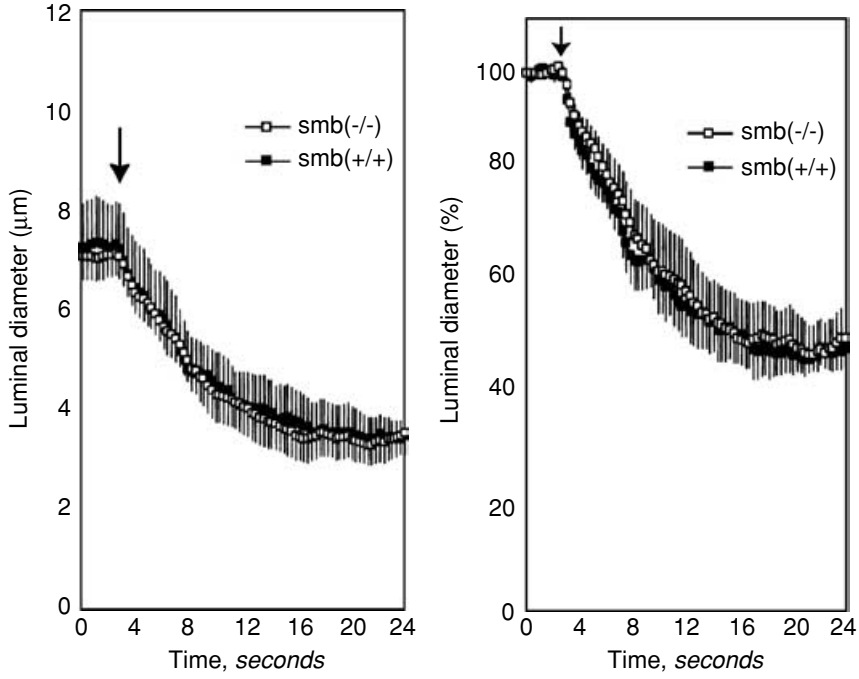

Fig. 3. Time courses of angiotensin II (Ang II) (10^{-8} mol/L)–induced constriction in efferent arterioles in smb(−/−) ($N = 8$) and smb(+/+) mice ($N = 6$). Absolute diameters (μm, left panel) did not differ significantly between both groups. There were no differences in the Ang II sensitivity (see relative changes of luminal diameters, right panel). The arrows indicate the start of the constriction. Data are presented as mean ± SEM.

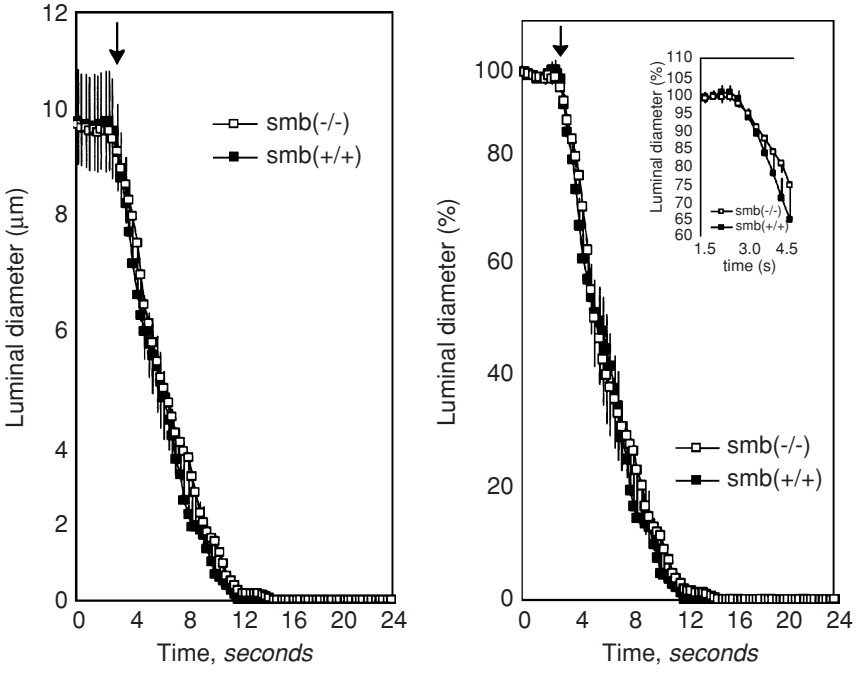

Fig. 4. Time courses of KCl (100 mol/L)–induced constriction in isolated, perfused afferent arterioles in smb(−/−) ($N = 11$) and smb(+/+) mice ($N = 9$). There were no differences in the course of the constriction between either the groups. The arrows indicate the start of the constriction. The inserted graph on the right panel demonstrates the courses for the beginning of the constriction in higher time and amplitude resolution. Data are presented as mean ± SEM.

smb(+/+) and smb(−/−) (Table 1). In addition, dc/dt_{max} of afferent arterioles was not significantly different from Ang II–induced constriction (Table 1).

Immunofluorescence analysis of SMB expression in renal arterioles

To detect the differential SMB expression in afferent and efferent arterioles of the mouse, and to demonstrate the absence of SMB expression in smb(−/−) mice, immunofluorescence microscopy of cryostat sections of kidneys dissected from smb(+/+) and smb(−/−) was performed using a double-labeling method. The specific antismooth muscle actin antibody was used to identify blood vessels, and the anti-SMB antibody was used for simultaneous detection of the SMB isoform expressed in the kidney vessels.

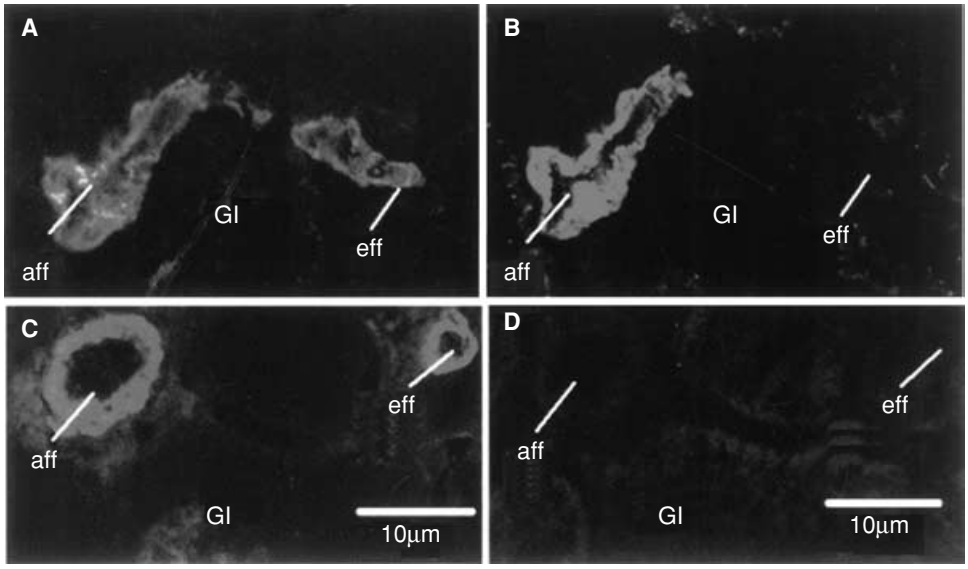

Fig. 5. Immunofluorescence micrographs of mouse kidneys of smb(+/+) (*A* and *B*) and smb(−/−) (*C* and *D*), double-labeled with anti-smooth muscle actin (0.5 μg/mL) (A and C) and anti-SMB (7.5 μg/mL) (B and D) antibodies. Primary antibodies were visualized with species-specific secondary antibodies conjugated with Alexa488 (A and C, green) and and Alexa594 (B and D, red). Abbreviations are: glom, glomerulus; aff, afferent arteriole; eff, efferent arteriole.

Afferent and efferent renal arterioles were stained with anti-smooth muscle actin in wild-type and SMB knockout animals (Fig. 5A and C). The types of renal blood vessels were identified according to their location (close to the glomerulus) and their wall thickness (afferent arterioles have a higher wall thickness than efferent arterioles). In wild-type mice, only afferent, but not efferent arterioles crossreacted with the anti-SMB antibody (Fig. 5B) demonstrating the differential expression pattern of SM-MHC isoenzymes in renal afferent and efferent arterioles. As expected, neither afferent nor efferent arterioles of smb(−/−) reacted with the SMB antibody (Fig. 5D).

Immuofluorescence analysis of renin expression in renal arterioles

Renin analysis of mouse kidneys obtained from smb(−/−) and smb(+/+) did not show significant differences. Total fluorescent area of smb(−/−) and smb(+/+) was 3340 ± 420 μm^2 and 3074 ± 921 μm^2, respectively. Average size of the fluorescent dots of smb(−/−) and smb(+/+) was 30.6 ± 4.8 μm^2, and 25.4 ± 5.02 μm^2, respectively. Area fraction of smb(−/−) and smb(+/+) was 1.25 ± 0.16% and 1.18 ± 0.35%, respectively. Values are means ± SEM of eight animals per groups.

DISCUSSION

Our results demonstrate that maximal constriction velocity (dc/dt_{max}) of mouse afferent arteriole upon Ang II was significantly higher than dc/dt_{max} of mouse efferent arteriole. A comparable result has also been observed with the corresponding rat arterioles [24]. The different contraction kinetics of afferent and efferent arterioles is in line with their physiologic function. Afferent arterioles regulate glomerular inflow resistance and have to constrict rapidly enough to balance fluctuations of systolic blood pressure. Efferent arterioles regulate glomerular outflow resistance, are not prone to rapid changes of blood pressure, and contract more tonically. In addition, we demonstrated that the mouse expressed SMB in renal afferent, but not efferent, arterioles, which is in close agreement with the rat renal blood vessels [24].

The aim of the present study was to investigate whether the different 5′-alternatively spliced smooth muscle myosin isoenzymes are causally related to the different contractile features of afferent and efferent arterioles. In fact, biochemical and kinetic properties of SMB [29, 31, 32] as well as some observations during physiologic experiments [22, 31, 33] may predict a higher constriction velocity of afferent compared to efferent arterioles.

The results of our study presented herein, however, suggest that the expression of 5′-inserted smooth muscle myosin may not be related to the higher contractile features of mouse afferent compared to efferent arterioles, as suggested previously [24]: we clearly show that the constriction amplitude, $t_{1/2,}$ and dc/dt_{max} values of afferent arterioles under physiologic load upon Ang II and KCl activation remain similar in normal and homozygous SMB knockout mice.

We cannot exclude completely that compensatory mechanisms, which are frequently observed in gene targeting studies (e.g., up-regulation or differential expression of regulatory thin filament proteins or MLC17

isoforms [c.f., 34]) could have balanced the predicted inhibitory effect of SMB ablation on renal arteriole constriction. Such a hypothetical compensatory mechanism, however, must then be focused selectively on the afferent arteriole since the contractile features of efferent arterioles remain similar in both smb (+/+) and smb(−/−). Furthermore, changes of the normal expression of alternatively 3′-spliced SM-MHC isoforms could not account for our observations, since those myosin isoenzymes seems not to be associated with motor properties of myosin [15] or shortening velocity of smooth muscle preparations [16]. Thus, it is unlikely that compensatory mechanisms could have obscured the physiologic role of the deleted SMB in renal arterioles. Consequently, even in the absence of the highly active SMB isoenzyme, the physiologic function of afferent arterioles is maintained, which is in close agreement with the normal phenotype, organ functions, and life span of smb(−/−) mice [22, 34]. Indeed, the presence of fast SMB or slow SMA isoforms in smooth muscle is not necessarily associated with a correspondingly fast or slow contraction of smooth muscle preparations [14, 16, 32, 34, 35], suggesting that other factors could well dominate the effects of alternatively 5′-spliced myosins.

The reason for the absence of any effect of alternatively 5′-spliced smooth muscle myosin isoforms on contractile features of afferent arterioles is not completely clear. Please note, that we investigated constriction velocities under physiologic pressure load. However, alternatively 5′-spliced smooth muscle myosin isoforms (or any other myosin isoform) revealed large differences only in vitro [13, 20, 21] and in muscle in particular under unloaded conditions [22, 31, 33]. Investigating the force-velocity relationship of smooth muscle preparations with different amounts of SMB and SMA, however, revealed just marginal differences of shortening velocity under high load [31, 34]. Since we investigated contractile parameters of our arterial preparations under pressure load in a physiologic range, a dominant modulatory role of alternatively 5′-spliced myosin isoforms on the regulation of contraction velocity could not be expected.

Hence, alternatively 5′-spliced SM-MHC isoenzymes may not determine the different contractile features of efferent and afferent arterioles under physiologic conditions. Our observations contradict the suggestion that it is the SMB expression which confers the higher contractile state to afferent arterioles [24]. Rather, different microstructures and activation mechanisms of pre- and postglomerular arterioles could well be responsible for the different contractile properties. With the exception of the distal rennin-producing juxtaglomerular cells, afferent arterioles are densely covered by contractile smooth muscle cells which contain large amounts of myofilaments with abundant thick filaments. Efferent arterioles, in contrast, have a sparse layer of smooth muscle cells which revealed a few myofilaments associated with very small amounts of thick filaments [23, 36]. A functionally relevant substitution of SMCs by renin-producing noncontractile cells in afferent arterioles [c.f., 23] could be excluded, since renin remained unchanged in our preparations.

Thus, the ability of afferent arterioles to generate force may be much higher than of efferent arterioles. Since the velocity of shortening declines with the force a muscle has to generate [37], the velocity to shorten against a given load of efferent arterioles should indeed be much slower than afferent arterioles. Afferent arterioles, but not efferent arterioles, revealed a myogenic response, could be activated by KCl depolarization [29], and expressed voltage-gated T- and L-type Ca^{2+} channels [25, 26]. Ang II activates Ca^{2+} entry through depolarization and activation of voltage-gated Ca^{2+} channels in afferent arterioles, while in efferent arterioles Ang II stimulated Ca^{2+} influx without depolarization via store-operated Ca^{2+} influx [25]. Contraction activation of pre- and postglomerular arterioles by Ang II, therefore, is elicited by different cellular pathways which consequently confer different contraction properties.

CONCLUSION

The different SMC density and myofilament structures, as well as the different Ca^{2+} activation characteristics, rather than the expression of distinct alternatively spliced SM-MHC isoenzymes, may be the dominant determinants of the specific contractile features of afferent and efferent arterioles under physiologically loaded conditions.

ACKNOWLEDGMENTS

This work was supported by a grant from the Deutsche Forschungsgemeinschaft Mo 362/16-2 for IM, HL-38355-17 (for M.P.), and AHA 0365173B (for G.J.B.). We greatly appreciate the technical assistance of Uta Stangenberg and Petra Pierschalek. We also would like to thank Dr. Gudrun Lutsch for her help in immunofluorescence.

Reprint requests to Ingo Morano, Ph.D., Max Delbrück Centrum for Molecular Medicine, Molecular Muscle Physiology, Robert-Rössle-Str. 10, 13122 Berlin, Germany.
E-mail: imorano@mdc-berlin.de

REFERENCES

1. Dominguez R, Freyzon Y, Trybus KM, Cohen C: Crystal structure of a vertebrate smooth muscle myosin motor domain and its complex with the essential light chain: Visualization of the pre-power stroke state. *Cell* 94:559–571, 1998
2. Rayment I, Rypniewski WR, Schmidt-Bäse K, *et al*: Three-dimensional structure of myosin subfragment 1: A molecular motor. *Science* 261: 50–58, 1993
3. Gaylinn BD, Eddinger TJ, Martino PA, *et al*: Expression of non-muscle myosin heavy and light chains in smooth muscle. *Am J Physiol* 257: C997–C1004, 1989
4. Packer CS: Arterial muscle myosin heavy chains and light chains in spontaneous hypertension. *Comp Biochem Physiol* 117B:19–28, 1997

5. Phillips CL, Yamakawa K, Adelstein RS: Cloning of the cDNA encoding nonmuscle myosin heavy chain-B and analysis of human tissues with isoform-specific antibodies. *J Muscle Res Cell Mot* 16:390–400, 1995
6. Deng Z, Liu P, Claxton DF, *et al*: Smooth muscle myosin heavy chain locus (MYH11) maps to 16p13.13-p13.12 and establishes a new region of conserved synteny between human 16p and mouse 16. *Genomics* 18:156–159, 1993
7. Morano I, Chai GX, Baltas LG, *et al*: Smooth muscle contraction without smooth muscle myosin. *Nature Cell Biol* 2:371–375, 2000
8. Loefgren M, Ekblad E, Morano I, Arner A: Nonmuscle myosin motor of smooth muscle. *J Gen Physiol* 121:301–310, 2003
9. Rovner AS, Freyzon Y, Trybus KM: An insert in the motor domain determines the functional properties of expressed smooth muscle myosin isoforms. *J Muscle Res Cell Motil* 18:103–110, 1997
10. Nagai R, Kuro-OM, Babij P, Periasamy M: Identification of two types of smooth muscle myosin heavy chain isoforms by cDNA cloning and immunoblot analysis. *J Biol Chem* 264:9734–9737, 1989
11. Hamada Y, Yanagisawa M, Katsugarawa Y, *et al*: Distinct vascular and intestinal smooth muscle myosin heavy chain mRNAs are encoded by a single-copy gene in the chicken. *Biochem Biophys Res Commun* 170:53–58, 1990
12. Babij P: Tissue-specific and developmentally regulated alternative splicing of a visceral isoform of smooth muscle myosin heavy chain. *Nucl Acid Res* 21:1467–1471, 1993
13. Kelley CA, Takahashi M, Yu JH, Adelstein RS: An insert of seven amino acids confers enzymatic differences between smooth muscle myosins from the intestines and vasculature. *J Biol Chem* 268:12848–12854, 1993
14. White S, Martin A, Periasamy M: Identification of a novel smooth muscle myosin heavy chain cDNA: Isoform diversity in the S1 head region. *Am J Physiol* 264:C1252–C1258, 1993
15. Kelley CA, Sellers JR, Goldsmithz PK, Adelstein RS: Smooth muscle myosin is composed of homodimeric heavy chains. *J Biol Chem* 267:2127–2130, 1992
16. Morano I, Erb G, Sogl B: Expression of myosin heavy and light chains changes during pregnancy in the rat uterus. *Pflügers Arch* 423:434–441, 1993
17. Siemankowski RF, Wiseman MO, White HD: ADP dissociation from actomyosin subfragment 1 is sufficient slow to limit the unloaded shortening velocity in vertebrate muscle. *Proc Natl Acad Sci* 82:658–662, 1985
18. Sweeney HL, Rosenfeld SS, Brown F, *et al*: Kinetic tuning of myosin via a flexible loop adjacent to the nucleotide binding pocket. *J Biol Chem* 273:6262–6270, 1998
19. Guilford WH, Dupuis DE, Kennedy G, *et al*: Smooth and skeletal muscle myosins produce similar unitary forces and displacements in the laser trap. *Biophys J* 72:1006–1021, 1997
20. Rovner AS, Thompson MM, Murphy RA: Two different myosin heavy chains are found in smooth muscle. *Am J Physiol* 250:C861–C870, 1986
21. Lauzon A-M, Tyska MJ, Rovner AS, *et al*: A 7-amino-acid insert in the heavy chain nucleotide binding loop alters the kinetics of smooth muscle myosin in the laser trap. *J Muscle Res Cell Mot* 19:825–837, 1998
22. Babu GJ, Loukianov E, Loukianova T, *et al*: Loss of SMB myosin affects muscle shortening velocity and maximal force development. *Nature Cell Biol* 3:1025–1029, 2001
23. Kimura K, Nagai R, Sakai T, *et al*: Diversity and variability of smooth muscle phenotypes of renal arterioles as revealed by myosin isoform expression. *Kidney Int* 48:372–382, 1995
24. Shiraishi M, Wang X, Walsh MP, *et al*: Myosin heavy chain expression in renal afferent and efferent arterioles: Relationship to contractile kinetics and function. *FASEB J* 17:2284–2296, 2003
25. Loutzenhiser K, Loutzenhiser R: Angiotensin II-induced Ca2+ influx in renal afferent and efferent arterioles: Differing roles of voltage-gated and store-operated Ca^{2+} entry. *Circ Res* 87:551–557, 2000
26. Hansen PB, Jensen BL, Andreasen D, Skott O: Differential expression of T- and L-type voltage-dependent calcium channels in renal resistance vessels. *Circ Res* 89:630–638, 2001
27. Patzak A, Lai EY, Mrowka R, *et al*: AT1 receptors mediate angiotensin II induced release of nitric oxide in afferent arterioles. *Kidney Int* 66:1949–1958, 2004
28. Carmines PK, Fowler BC, Bell PD: Segmentally distinct effects of depolarization on intracellular [Ca2+] in renal arterioles. *Am J Physiol Renal Physiol* 265:F677–F685, 1993
29. Loutzenhiser K, Hayashi K, Epstein M: Divergent effects of KCI-induced depolarization on afferent and efferent arterioles. *Am J Physiol* 257:F561–F564, 1989
30. Wetzel U, Lutsch G, Haase H, *et al*: Alternative splicing of smooth muscle myosin heavy chain in cardiac vessels of normotensive and hypertensive rats. *Circ Res* 83:204–209, 1998
31. Sjuve R, Haase H, Morano I, *et al*: Contraction kinetics and myosin isoform composition in smooth muscle from hypertrophied rat urinary bladder. *J Cell Biochem* 63:86–93, 1996
32. Malmqvist U, Arner A: Correlation between isoform composition of the 17 kDa myosin light chain and maximal shortening velocity in smooth muscle. *Pflügers Arch* 418:423–530, 1991
33. Tuck SA, Maghni K, Poirier A, *et al*: Time course of airway mechanics of the (+)insert myosin isoform knockout mouse. *Am J Respir Cell Mol Biol* 30:326–323, 2003
34. Babu GJ, Pyne GJ, Zhou Y, *et al*: Isoform switching from SMB toSMA myosin results in decreased contractility and altered isoform expression of thin filament regulatory prteins. *Am J Physiol cell Physiol* 287:C723–C729, 2004
35. Siegman MJ, Butler TM, Mooers SU, *et al*: Hypertrophy of colonic smooth muscle: contractile proteins, shortening velocity, and regulation. *Am J Physiol* 272:G1571–G1580, 1997
36. Gattone VH, Luft FC, Evan AP: Renal afferent and efferent arterioles of the rabbit. *Am J Physiol* 16:F219–F228, 1984
37. Hill AV: The heat of shortening and the dynamic constants of muscle. *Proc Royal Soc B* 126:136–195, 1938